Chalcones as Environmentally-Friendly Corrosion Inhibitors for Stainless Steel Type 304 in 1 M HCl Solutions

A.S.Fouda [1,*], A.F.Hassan [2], M.A.Elmorsi [3], T.A.Fayed [3] and A.Abdelhakim [3]

[1]Department of Chemistry, Faculty of Science, El-Mansoura University, El-Mansoura-35516, Egypt:
[2]Department of Chemistry, Faculty of Science, Damanhur University, Damanhur- Egypt
[3]Department of Chemistry, Faculty of Science, Tanta University, Egypt
[*]E-mail: asfouda@hotmail.com

The effect of Chalcones on the corrosion behavior of SS type 304 in 1 M HCl solution has been investigated by weight loss, potentiodynamic polarization, electrochemical impedance spectroscopy (EIS)and Electrochemical frequency modulation (EFM) techniques. The inhibition efficiency increased with increase in inhibitor concentration but decreased with increase in temperature. The thermodynamic parameters of corrosion and adsorption processes were calculated and discussed. The adsorption of these inhibitors on the surface of SS type 304 in 1 M HCl was found to obey Langmuir adsorption isotherm. The potentiodynamic polarization measurements indicated that the inhibitors are of mixed type. The morphology of inhibited SS type 304 was analyzed by scanning electron microscope technology with energy dispersive X-ray spectroscopy ((SEM–EDX). Electrochemical impedance was used to investigate the mechanism of corrosion inhibition. The presence of these compounds in the solution decreases the double layer capacitance and increases the charge transfer resistance.The results obtained from the three different techniques were in good agreement. Quantum structure-activity relationships have been used to study the effect of molecular structure on inhibition efficiency of the inhibitors.

1. INTRODUCTION

Stainless steel is a material frequently used due to its properties of resistance to corrosion in both the industrial domain and the maritime field. The most important fields of applications being acid pickling, industrial acid cleaning, acid descaling and oil well acidizing. Indeed, in contact with the air, the surface is quickly covered with a chromium and iron oxide layer, which increases the resistance to corrosion. SS type 304 was chosen in this study because of its frequent use and its relatively weak

resistance to corrosion, allowing assessing more easily the influence of the environment on corrosion. It is possible to reduce the corrosion rate to safe level by adding inhibitors. Organic compounds and their derivatives were used successfully as inhibitors for different types of steels and were studied extensively through the last century. Recently, interest is still growing for exploiting other inhibitors for the corrosion of stainless steels [1]. Several organic molecules containing sulfur, oxygen and nitrogen hetero-atoms were suggested as inhibitors for steel in acidic medium [2-8]. The inhibition mechanism for this class of inhibitors is mainly based on adsorption [9].

The present investigation aimed to: i) study the effect of Chalcones as environmentally-friendly corrosion inhibitors for the corrosion of SS type 304 in 1 M HCl, ii)compare the corrosion inhibition data derived from EFM with that obtained from Tafel extrapolation, EIS and weight loss techniques, iii) Study the surface morphology by SEM and EDX techniques iv) discuss the relationship between calculated quantum chemical parameters and experimental inhibition efficiencies of the inhibitors.

2. EXPERIMENTAL METHODS

2.1. Materials

The experiments were performed with stainless steel type 304specimens in the form of rods and sheets with the following composition in Table (1):

Stainless steel type								
	C	Mn	P	S	Si	Cr	Ni	**Fe**
304	**0.08**	**2.0**	**0.04**	**0.03**	**0.75**	**18-20**	**8-11**	**rest**

All chemicals and reagents used are with analytical grade and used without further purification.

2.2. Solutions

The aggressive solutions used were made of AR grade HCl. Appropriate concentrations of acid were prepared using bidistilled water. 10^{-3}M stock solutions from the investigated compounds were prepared by dissolving the appropriate weights of the used chemically pure solid compounds in absolute ethanol.

2.3. Weight loss method

Three parallel stainless steel sheets of 2 x 2 x 0.2 cm were abraded with emery paper up to 1200 grit, washed with bidistilled water and acetone. After weighing accurately, the specimens were immersed in 100 ml beaker, which contained 100 ml 1 M HCl with and without addition of different

concentrations of inhibitors at 25±1°C. The test specimens were suspended by suitable glass hooks at the edge of the basin, and under the surface of the test solution by about 1cm. All the aggressive acid solutions were open to air. After specified immersion time, the specimens were taken out, washed, dried, and weighed. The average weight loss of the three parallel stainless steel sheets could be obtained. Then the tests were prepared at different temperatures. The inhibition efficiency (% IE) and the degree of surface coverage (θ) of investigated inhibitors on the corrosion of SS were calculated from the following equation [10]:

$$\% \text{ IE} = \theta \times 100 = [(W_o - W)/ W_o] \times 100 \qquad (1)$$

Where W_o and W are the values of the average weight losses without and with addition of the inhibitor, respectively.

2.4. Potentiodynamic polarization measurements

Polarization experiments were carried out in a conventional three-electrode cell with a platinum counter electrode (1 cm^2) and a saturated calomel electrode (SCE) coupled to a fine Luggin capillary as the reference electrode. The working electrode was in the form of a square cut from stainless steel sheet (1 x 1 cm)embedded in epoxy resin of polytetrafluoroethelene so that the flat surface was the only surface in the electrode. Before polarization scanning, working electrode was immersed in the test electrolyte of 100 ml in volume for 30 min until steady state and the open circuit potential (OCP) was attained which was taken as E_{OC}. All experiments were carried out at 25 ±1°C using Lab companion circulator thermostat and solutions were not dearated. For polarization measurements potential from -350 to 100 mV (relative to open circuit potential, E_{OC}) was applied while potential from -500 to 700 mV (relative to reference electrode potential, E_{ref}) was applied in case of pitting measurements. % IE and the degree of surface coverage (θ) were calculated from the following equation:

$$\% \text{ IE} = \theta \times 100 = [(i_{corr} - i_{corr(inh)}) / i_{corr}] \times 100 \qquad (2)$$

Where i_{corr} and $i_{corr(inh)}$ are the uninhibited and inhibited corrosion current density values, respectively, determined by extrapolation of Tafel lines to the corrosion potential.

2.5. Electrochemical impedance spectroscopy measurements

The EIS spectra were recorded at open circuit potential (OCP) after immersion the electrode for 30 min in the test solution. The AC signal was 5 mV peak to peak and the frequency range studied was between 100 kHz and 0.2 Hz. The inhibition efficiency (% IE) and the surface coverage (θ) of the used inhibitors obtained from the impedance measurements can be calculated by applying the following equation:

$$\% \text{ IE} = \theta \times 100 = [1 - (R^{\circ}_{ct}/R_{ct})] \qquad (3)$$

Where R^o_{ct} and R_{ct} are the charge transfer resistance in the absence and presence of inhibitor, respectively.

2.6. Electrochemical frequency modulation measurements

EFM experiments were performed with applying potential perturbation signal with amplitude 10 mV with two sine waves of 2 and 5 Hz. The choice for the frequencies of2 and 5Hz was based on three arguments [11]. The larger peaks were used to calculate the corrosion current density (i_{corr}), the Tafel slopes (βc and βa) and the causality factors CF2 and CF3 [12].

All electrochemical experiments were carried out using Gamry instrument PCI300/4 Potentiostat/Galvanostat/Zra analyzer, DC105 software for polarization, EIS 300 for electrochemical impedance spectroscopy software, EFM140 for electrochemical frequency modulation software and Echem Analyst 5.5 for results plotting, graphing, data fitting and calculating.

2.7. SEM-EDX Measurements

SS type 304 surfaces was prepared by keeping the specimens for 3days in 1 M HCl in presence and absence of optimum concentration of Chalcones derivative, after abraded mechanically using different emery papers up to 1200 grit size. Then, after this immersion time, the specimens were washed gently with distilled water, carefully dried and mounted into the spectrometer without any further treatment.
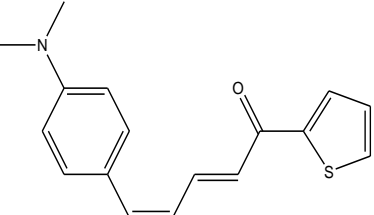
The corroded alloy surfaces were examined using an X-ray diffractometer Philips (pw-1390) with Cu-tube (Cu Ka1, l = 1.54051 A °), a scanning electron microscope (SEM, JOEL, JSM-T20, Japan).

2.8. Theoretical study

Accelrys (Material Studio Version 4.4) software for quantum chemical calculations has been used.

2.9. Inhibitors

Table 2. Chemical structures, names, molecular formulas and molecular weights of Chalcone are given in Table 2 and were prepared as before [13]:

Comp	Structure	Name	Mol. Wt. / Mol. Formula
1		(2E,4Z)-5-(4-(dimethylamino)phenyl)-1-(thiophene-2-yl)penta-2,4-dien-1-one	$C_{17}H_{17}NOS$ 283.39

| 2 | | (2E,4Z)-5-(4-(dimethylamino)phenyl)-1-(furan-2-yl)penta-2,4-dien-1-one | $C_{17}H_{17}NO_2$ 267.32 |
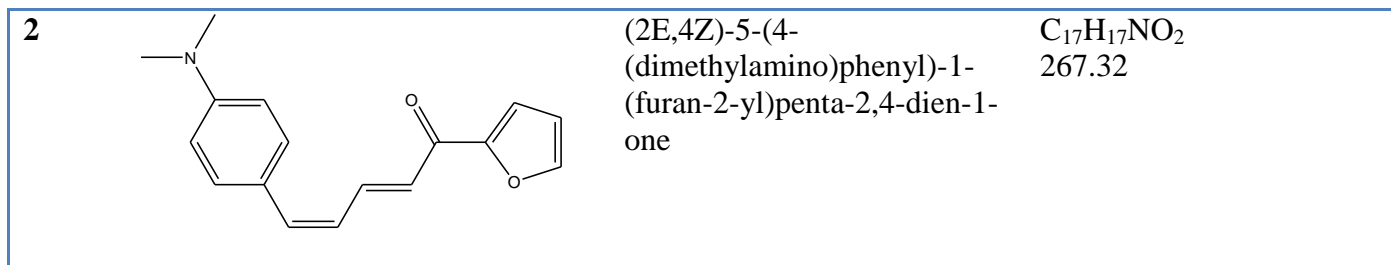
3. RESULTS AND DISCUSSION

3.1. Weight loss measurements

The weight losses of SS type 304 specimens in 1 M HCl solution, without and with different concentrations from the investigated inhibitors, were determined at different times of immersion at 25°C. Figure 1 represents the weight loss of SS type 304 in 1 M HCl solutions, without and with different concentrations of compound (1) as an example. Similar curves were obtained for compound (2) (not shown). The presence of inhibitors reduces the corrosion rate of steel in HCl. Values of % IE are tabulated in Table (3). In all cases, the increase in the inhibitor concentration was accompanied by a decrease in the weight loss and an increase in % IE. These results lead to the conclusion that, these compounds under investigation are fairly efficient inhibitors for SS type 304 dissolution in HCl solution. Careful inspection of these results showed that, at the same inhibitor concentration, the ranking of the inhibitors according to % IE is as follow: compound (1) > compound (2)

Table 3. Variation of inhibition efficiency (%IE) of different compounds (1 and 2) with their molar concentrations from weight loss measurements at 120 min immersion in 1 M HCl at 25°C

Conc., M	inhibition efficiency (% IE)	
	Compound (1)	Compound (2)
1×10^{-6}	64.3	62.2
5×10^{-6}	69.4	66.6
10×10^{-6}	73.3	70.9
15×10^{-6}	77.0	73.6
20×10^{-6}	80.8	77.4
25×10^{-6}	86.4	83.7
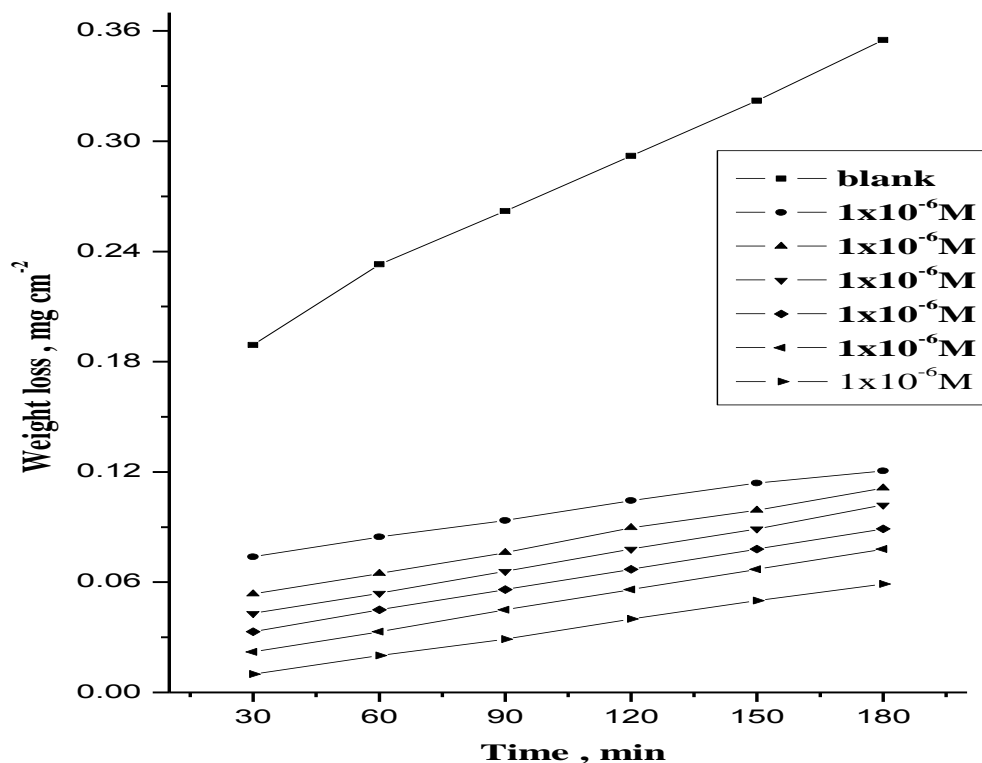
Figure 1. Weight loss-time curves for the corrosion of SS type 304 in 1 M HCl in the absence and presence of different concentrations of compound (1) at 25 ^{o}C

3.1.1 Adsorption isotherm

One of the most convenient ways of expressing adsorption quantitatively is by deriving the adsorption isotherm that characterizes the metal/inhibitor/ environment system [14].Various adsorption isotherms were applied to fit θ values but the best fit was found to obey Langmuir adsorption isotherm [15] which may be expressed by:

$$C/\theta = 1/K_{ads} + C \qquad (4)$$

where C is inhibitor concentration and K_{ads} is equilibrium constant of adsorption. It is well known that the standard adsorption free energy ($\Delta G°_{ads}$) is related to equilibrium constant of adsorption (K_{ads}) by the following equation [16]:

$$K_{ads} = 1/55.5 \exp [-\Delta G°_{ads}/RT] \qquad (5)$$

Figures (2&3) represent the plot of (C/θ) against C for all investigated compounds for the corrosion of SS type 304 in 1M HCl at 25°C. As can be seen from t6hese Figures the Langmuir isotherm is the best one which explains the experimental results. The values of K_{ads} and $\Delta G°_{ads}$ calculated from Langmuir isotherms are given in Table (4). The negative values of $\Delta G°_{ads}$ suggested that the adsorption of inhibitors molecules onto SS surface is a spontaneous process. The magnitude of heat of adsorption reaches the magnitude of heat of chemical reaction, which is the result of the transference of electron from donating atoms in the inhibitor molecule to the d-orbital of the iron atom. This means that the given inhibitor molecules will form monolayer on the steel surface. In general the

values of ΔG°_{ads} obtained from Langmuir isotherms and the equilibrium constant of adsorption of inhibitors decreases in the order: compound (1) > compound (2).
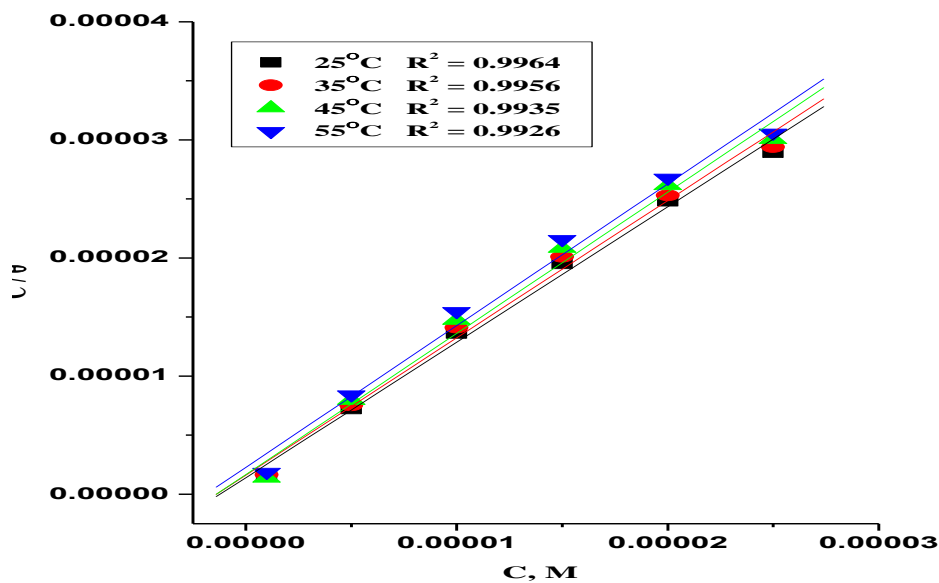
Figure 2. Langmuir adsorption isotherm of compound (1) on SS type 304 surface in 1 M HCl at different temperatures
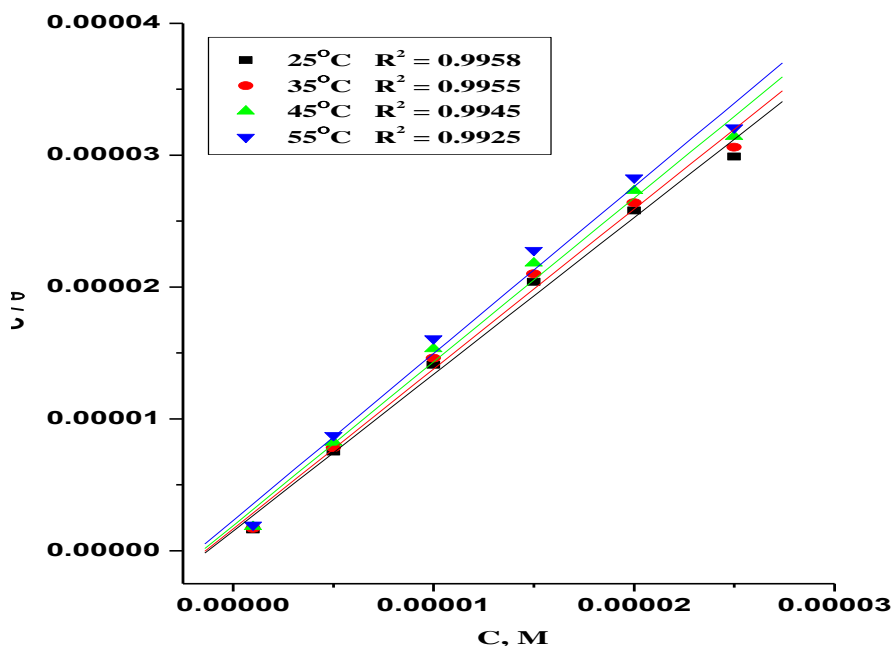
Figure 3. Langmuir adsorption isotherm of compound (2) on SS type 304 surface in 1 M HCl at different temperatures

3.1.2. Thermodynamic adsorption parameters

The well-known thermodynamic adsorption parameters are the free energy of adsorption ($\Delta G°_{ads}$), the heat of adsorption ($\Delta H°_{ads}$) and the entropy of adsorption ($\Delta S°_{ads}$). These quantities can be calculated by various mathematical methods depending on the estimated values of K_{ads} from adsorption isotherm, at different temperatures as follows:

The $\Delta G°_{ads}$ values at all studied temperatures can be calculated from the following equation:

$$K_{ads} = (1/55.5) \exp(-\Delta G°_{ads}/RT) \qquad (6)$$

where 55.5 is the concentration of water in (M^{-1}) at metal\solution interface. The heat of adsorption ($\Delta H°_{ads}$) could be calculated according to the Van't Hoff equation:

$$LogK_{ads} = (-\Delta H°_{ads}/2.303RT) + constant) \qquad (7)$$

In order to calculate heat of adsorption ($\Delta H°_{ads}$), log K_{ads} was plotted against $1/T$ as shown in Figures (2 & 3). The straight lines were obtained with slope equal to ($-\Delta H°_{ads}/R$). Then in accordance with the basic equation:

$$\Delta G°_{ads} = \Delta H°_{ads} - T\Delta S°_{ads} \qquad (8)$$

By introducing the obtained $\Delta G°_{ads}$ and $\Delta H°_{ads}$ values in equation (8), the entropy of adsorption ($\Delta S°_{ads}$) values were calculated at all studied temperatures. All estimated thermodynamic adsorption parameters for the studied compounds on SS type 304 from 1 M HCl solution were listed in Tables (4).

Table 4. Thermodynamic parameters for the adsorption of compounds (1) and (2) on SS type 304 surface in 1 M HCl at different temperatures

Comp.	Temperature, °C	$-\Delta G°_{ads}$, kJ mole^{-1}	$-\Delta H°_{ads}$, kJ mol^{-1}	$-\Delta S°_{ads}$ J mol^{-1} k^{-1}	K_{ads}, M^{-1}x10^{-4}
1	25	46.4	11.8	105.7	**71.6**
	35	45.8		105.8	**62.1**
	45	44.4		106.8	**60.4**
	55	43.3		105.3	**44.2**
2	25	46.3	11.6	105.8	**67.2**
	35	45.4		106.2	**60.5**
	45	44.3		106.2	**52.5**
	55	43.2		105.8	**43.6**

Inspection of the obtained data, it was found that: The negative values of $\Delta G°_{ads}$ reflect that the adsorption of studied inhibitors on SS type 304 surface from 1 M HCl solution is spontaneous process. $\Delta G°_{ads}$ values increase (become less negative) with an increase of temperature which indicates the occurrence of exothermic process at which adsorption was unfavorable with increasing reaction temperature as the result of the inhibitor desorption from the SS type 304 surface. It is usually accepted that the value of $\Delta G°_{ads}$ around 20 kJ mol^{-1} or lower indicates the electrostatic interaction between charged metal surface and charged organic molecules in the bulk of the solution while those around -40 kJ mol^{-1} or higher involve charge sharing or charge transfer between the metal surface and organic

molecules. From the obtained values of $\Delta G°_{ads}$ it was found the existence of comprehensive (physical and chemical adsorption). The negative sign of $\Delta H°_{ads}$ reveals that the adsorption of inhibitor molecules is an exothermic process. Generally, an exothermic adsorption process suggests either physisorption or chemisorption while endothermic process is attributed to chemisorption. The unshared electron pairs in investigated molecules may interact with d-orbitals of SS type 304 to provide a protective chemisorbed film. In the case of investigated compounds, the absolute values of enthalpy are relatively low, approaching those typical of physisorption. The values of $\Delta S°_{ads}$ in the presence of inhibitors are large and negative that is accompanied with exothermic adsorption process.

3.1.2. Kinetic parameters

The effect of temperature on the inhibited acid-metal reaction is highly complex, because many changes occur on the metal surface, such as rapid etching and desorption of the inhibitor and the

Generally the corrosion rate increases with the rise of temperature. It was found that the inhibition efficiency decreases with increasing temperature and increases with increasing the concentration of the inhibitor. The activation energy (E^*_a) of the corrosion process was calculated using Arrhenius equation [17]:

$$k_{corr} = A \exp (-E^*_a / RT) \qquad (9)$$

where k_{corr} is corrosion rate and A is Arrhenius constant. The values of activation energies E^*_a can be obtained from the slope of the straight lines of plotting log k_{corr} vs 1/T in the presence and absence of investigated compounds at various temperatures [Figure (4)] and are given in Table (5). It is noted that the values of activation energy increase in the presence of inhibitors and with increase of the concentration of the inhibitors. This is due to the formation of a film of inhibitors on SS type 304surface. The activation energy for the corrosion of SS type 304 in 1 M HCl was found to be 50.4 kJ mol^{-1} which is in good agreement with the work carried out by others [18-19]. An alternative formulation of the Arrhenius equation is the transition state equation [20]:

$$k_{corr} = RT/Nh \exp (\Delta S^*/R) \exp (-\Delta H^* / RT) \qquad (10)$$

where h is Planck's constant, N is Avogadro's number, ΔS^* is the entropy of activation and ΔH^* is the enthalpy of activation. Figure (5) shows a plot of log (k_{corr} / T) vs. (1/T). Straight lines are obtained with a slope of $(\Delta H^*/2.303 R)$ and an intercept of (log R/Nh + $\Delta S^*/2.303 R)$ from which the values of ΔH^* and ΔS^* are calculated and also listed in Table (5). From inspection of Table (5) it is clear that the positive values of ΔH^* reflect that the process of adsorption of the inhibitors on the SS surface is an endothermic process and not approach 100 kJ mol^{-1} [21] i.e. These compounds adsorbed physically on SS surface. More interesting behavior was observed in Table (5) that positive ΔS^* values is accompanied with endothermic adsorption process. This is agrees with what expected, when the adsorption is an endothermic process, it must be accompanied by an increase in the entropy energy change and vies versa [22]. It is seen that investigated derivatives have inhibiting properties at all the studied temperatures and the values of % IE decrease with temperature increase. This shows that there is a desorption of the molecules from the SS surface with increase in temperature.
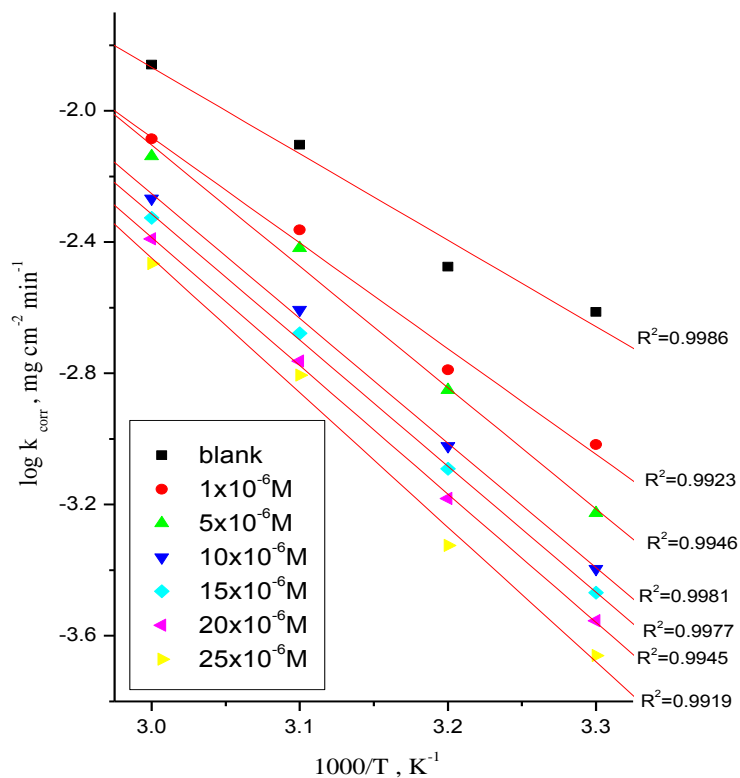
Figure 4. Arrhenius plots for SS type 304 corrosion rates (k$_{corr.}$) after 120 minutes of immersion in 1 M HCl in the absence and presence of different concentrations of compound (1)
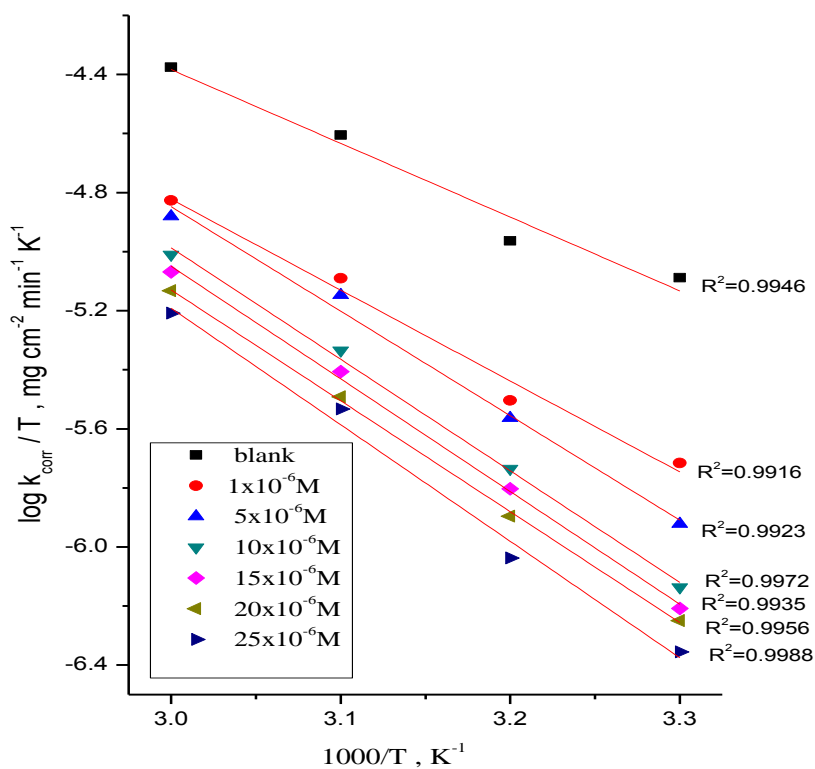
Figure 5. Plots of (log k$_{corr}$/T)vs.1/T for corrosion of SS type 304 in 1M HCl in the absence and presence of different concentrations of compound (1)

Table 5. Activation parameters for the dissolution of SS type 304 in the presence and absence of different concentrations of compounds (1) and (2) in 1 M HCl

| Inhibitor	Conc.,x 10^{-6} M	Activation parameters		
		E_a^*	ΔH^*	ΔS^*
		$kJ\ mol^{-1}$	$kJ\ mol^{-1}$	$J\ mol^{-1}\ K^{-1}$
Free Acid 1M HCl	0.0	50.4	20.2	139.6
1	1	61.7	25.0	114.7
	5	70.8	28.8	88.4
	10	72.8	30.5	81.9
	15	73.5	30.7	77.5
	20	74.9	31.0	76.5
	25	78.6	32.0	72.1
2	1	56.6	22.6	125.3
	5	64.9	26.2	100.7
	10	66.7	27.0	97.7
	15	67.5	27.2	97.0
	20	68.7	27.7	94.9
	25	72.1	30.0	79.9

3.2. Potentiodynamic polarization

Anodic and cathodic polarizations were carried out potentiodynamic in unstirred 1.0 M HCl solution in the absence and presence of various concentrations of the inhibitors (1- 2) at 25 °C over potential range 300 mV ± OCP. The results are represented in Figure (6) for compound (1), similar behaviors were obtained for other compound (not shown). The obtained potentiodynamic polarization parameters are given in Table (6). These results indicate that the cathodic and anodic curves obtained exhibit Tafel-type behavior. Additionally, the form of these curves is very similar either in the cathodic or in the anodic side, which indicates that the mechanisms of SS type 304dissolution and hydrogen reduction apparently remain unaltered in the presence of these additives. Addition of inhibitors decreased both the cathodic and anodic current densities and caused mainly parallel displacement to the more negative and positive values, respectively, i.e. the presence of tested derivatives in solution inhibit both the hydrogen evolution and the anodic dissolution processes with overall shift of E_{corr} to more negative values with respect to the OCP. The results also show that the slopes of the anodic and the cathodic Tafel slopes (β_a and β_c) were slightly changed on increasing the concentration of the tested compounds. This could be interpreted as an action of mixed inhibitor control over the electrochemical semi-reactions. This means that the tested derivatives are mixed type inhibitors, but the cathode is more preferentially polarized than the anode. The higher values of Tafel slope can be attributed to surface kinetic process rather the diffusion-controlled process [23]. The constancy and the parallel of cathodic slope obtained from the electrochemical measurements indicate that the hydrogen evolution reaction was activation controlled [24] and the addition of these derivatives did not modify the mechanism of this process. This result suggests that the inhibition mode of the tested derivatives

used was by simple blockage of the surface by adsorption.

Table 6. The effect of concentration of the investigated compounds on the free corrosion potential (E_{corr}), corrosion current density (i_{corr}), Tafel slopes (β_a & β_c), degree of surface coverage θ, and inhibition efficiency (% IE) for the corrosion of SS type 304 in 1 M HCl at 25 ^{o}C

| Comp	Conc., x10⁶M	-E$_{corr.}$, mVvs SCE	i$_{corr}$, µA cm^{-2}	β$_a$, mV dec^{-1}	β$_c$, mV dec^{-1}	θ	% IE
	Blank	399	221.0	94	133	----	-----
1	1	391	62.5	46	107	0.717	71.7
	5	409	54.0	70	104	0.756	75.6
	10	408	48.4	66	100	0.781	78.1
	15	387	42.9	57	105	0.806	80.6
	20	406	31.5	52	90	0.857	85.7
	25	404	19.1	94	116	0.913	91.3
2	1	420	79.8	67	106	0.639	63.9
	5	391	61.6	45	107	0.721	72.1
	10	420	52.2	60	100	0.764	76.4
	15	408	49.2	67	101	0.777	77.7
	20	404	39.4	66	102	0.822	82.2
	25	405	25.7	73	107	0.883	88.3
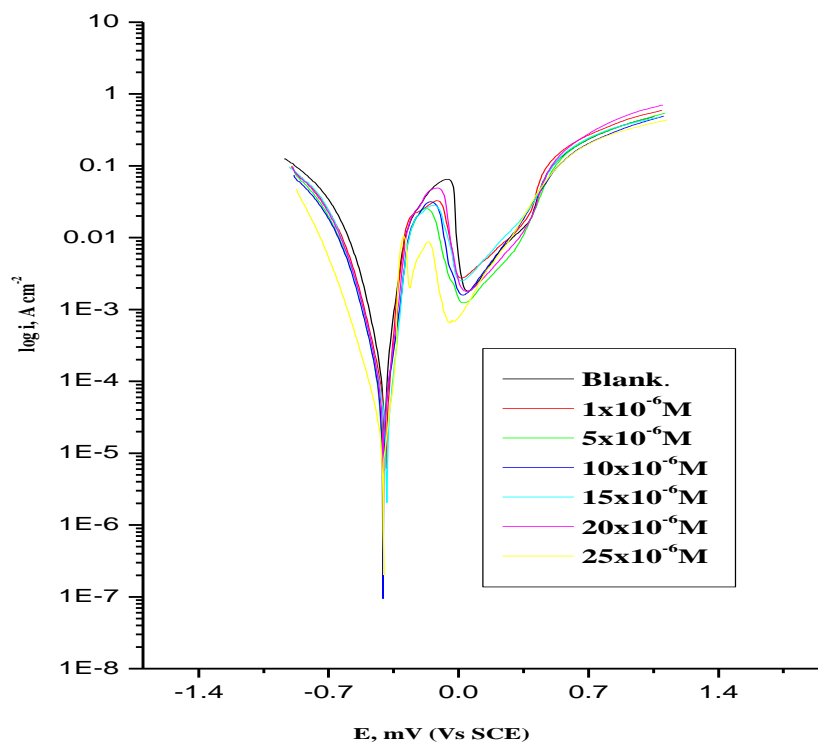
Figure 6. Potentiodynamic polarization curves for the corrosion of SS type 304 in 1 M HCl in the absence and presence of various concentrations of compound (1) at 25°C

*3.3. Electrochemical impedance spectroscopy measurements*

Impedance diagram (Nyquist) at frequencies ranging from 1 Hz to 1 kHz with 10 mV amplitude signal at OCP for SS type 304 in 1 M HCl in the absence and presence of different concentrations of compounds (1-2) are obtained. The equivalent circuit that describes our metal/electrolyte interface is shown in Figure (7) where R_s, R_{ct} and CPE refer to solution resistance, charge transfer resistance and constant phase element, respectively. EIS parameters and % IE were calculated and tabulated in Table (7). In order to correlate impedance and polarization methods, i_{corr} values were obtained from polarization curves and Nyquist plots in the absence and presence of different concentrations of compounds (1-2) using the Stern-Geary equation:

$$i_{corr} = \frac{\beta_a \beta_c}{2.303\,(\beta_a + \beta_c)\,R_{ct}} \tag{11}$$

The obtained Nyquist plot for compound (1) is shown in Figure (8). Each spectrum is characterized by a single full semicircle. The fact that impedance diagrams have an approximately semicircular appearance shows that the corrosion of SS type 304 is controlled by a charge transfer process. Small distortion was observed in some diagrams, this distortion has been attributed to frequency dispersion [25]. The diameters of the capacitive loop obtained increases in the presence of organic derivatives, and were indicative of the degree of inhibition of the corrosion process [26]. It was observed from the obtained EIS data that R_{ct} increases and C_{dl} decreases with the increasing of inhibitor concentrations. The increase in R_{ct} values, and consequently of inhibition efficiency, may be due to the gradual replacement of water molecules by the adsorption of the inhibitor molecules on the metal surface to form an adherent film on the metal surface, and this suggests that the coverage of the metal surface by the film decreases the double layer thickness. Also, this decrease of C_{dl} at the metal/solution interface with increasing the inhibitor concentration can result from a decrease in local dielectric constant which indicates that the inhibitors were adsorbed on the surface at both anodic and cathodic sites [27].
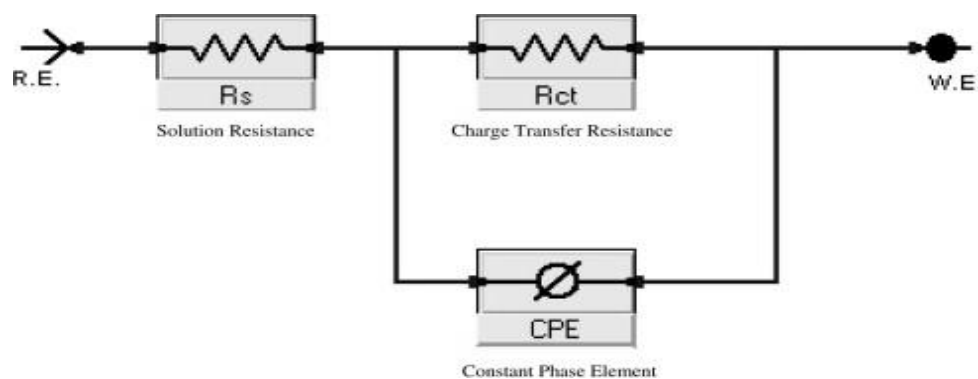
Figure 7. Equivalent circuit model used to fit experimental EIS
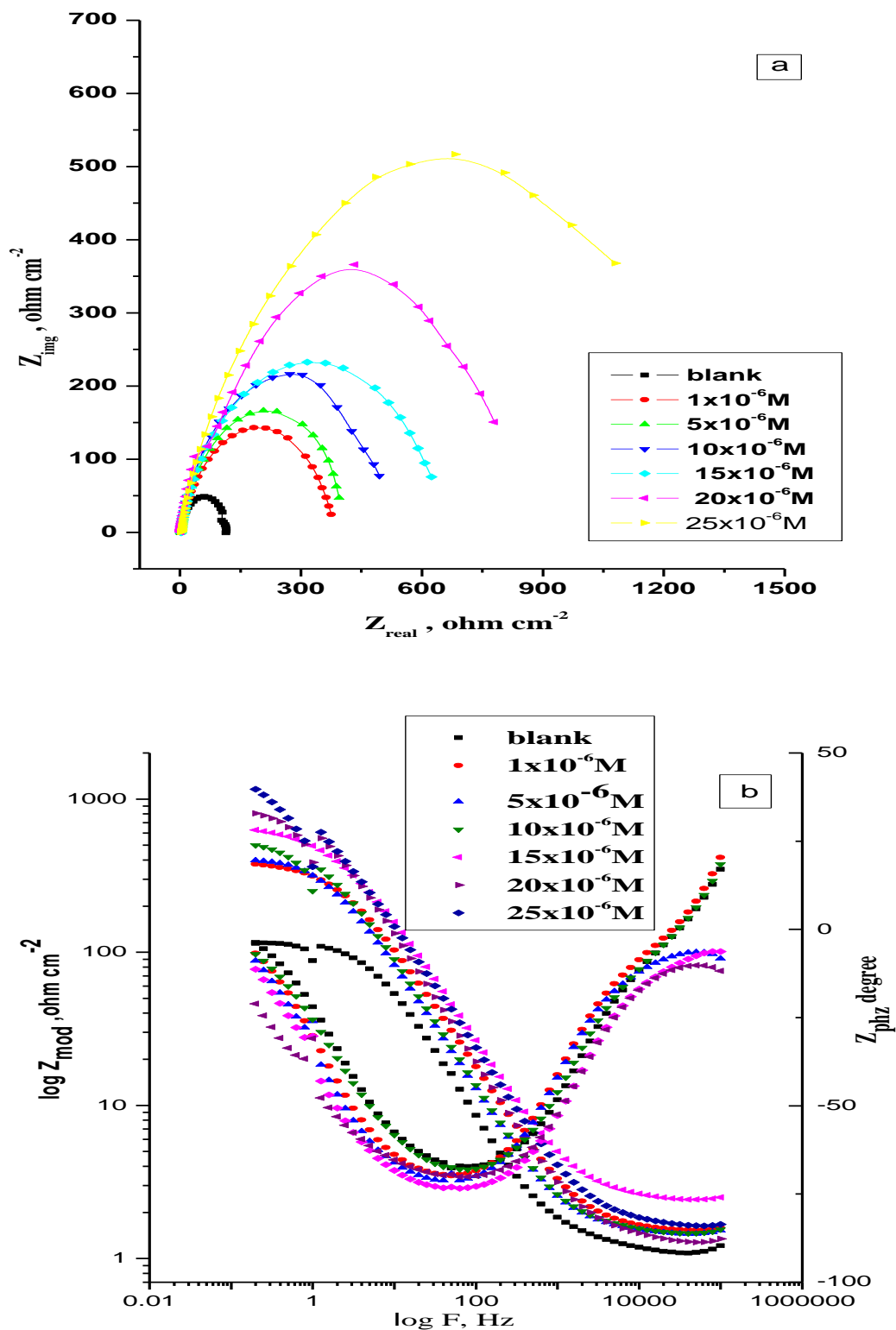
Figure 8. The Nyquist (a) and Bode (b) plots for corrosion of SS type 304 in 1 M HCl in the absence and presence of different concentrations of compound (1) at 25°C

The impedance data confirm the inhibition behavior of the inhibitors obtained with other techniques. From the data of Table (7), it can be seen that the i_{corr} values decrease significantly in the

presence of these additives and the % IE is greatly improved. The order of reduction in i_{corr} exactly correlates with that obtained from potentiostatic polarization studies. Moreover, the decrease in the values of i_{corr} follows the same order as that obtained for the values of C_{dl}. It can be concluded that the inhibition efficiency found from weight loss, polarization curves, electrochemical impedance spectroscopy measurements and the Stern-Geary equation are in good agreement.

Table 7. Electrochemical kinetic parameters obtained from EIS technique for SS type 304 in 1M HCl in the absence and presence of different concentrations of compounds 1 and 2 at 25°C

Comp.	Conc., M M	R_S, Ω cm^2	Y_o, x 10^{-6} $\mu\Omega^{-1}s^n$	n x10^{-3}	R_{ct} Ω cm^2	C_{dl}, x10^4 μ Fcm^{-2}	θ	% IE
1	Blank	1.148	412.5	876.1	113.7	2.67	-----	-----
	1x10^{-6}	1.518	274.9	829.6	378.8	2.41	0.700	70.0
	5x10^{-6}	1.464	342.2	847.7	419.4	2.31	0.729	72.9
	10x10^{-6}	1.472	324.1	846.3	483.3	1.83	0.765	76.5
	15x10^{-6}	2.417	189.1	827.3	628.1	1.72	0.819	81.9
	20x10^{-6}	1.285	221.4	849.7	786.3	1.62	0.855	85.5
	25x10^{-6}	1.562	255.5	800.2	1041	1.21	0.891	89.1
2	1x10^{-6}	1.645	292.4	836.3	307.6	1.89	0.630	63.0
	5x10^{-6}	1.443	306.4	823.3	347.4	1.82	0.673	67.3
	10x10^{-6}	1.262	274.3	827.8	384.4	1.71	0.704	70.4
	15x10^{-6}	1.452	198.3	845.9	504.2	1.30	0.774	77.4
	20x10^{-6}	1.444	176.7	828.7	657.1	1.22	0.827	82.7
	25x10^{-6}	1.326	125.4	823.9	872.5	1.11	0.870	87.0

*3.4. Electrochemical frequency modulation measurements (EFM)*

EFM is a nondestructive corrosion measurement technique that can directly and quickly determine the corrosion current value without prior knowledge of Tafel slopes, and with only a small polarizing signal. These advantages of EFM technique make it an ideal candidate for online corrosion monitoring [28].

The great strength of the EFM is the causality factors which serve as an internal check on the validity of EFM measurement. The causality factors CF-2 and CF-3 are calculated from the frequency spectrum of the current responses. Figure (9) shows the frequency spectrum of the current response of pure SS type 304 in 1 M HCl. The EFM intermodulation spectrums of pure SS type 304 in 1 M HCl acid solution containing (1x10^{-5} M and 25x10^{-5} M) of the studied inhibitors are shown in Figure (9). Similar results were recorded for the other concentrations of the investigated compounds (not shown). The experimental EFM data were treated using two different models: complete diffusion control of the cathodic reaction and the "activation" model. For the latter, a set of three non-linear equations had been solved, assuming that the corrosion potential does not change due to the polarization of the working electrode [29]. The larger peaks were used to calculate the corrosion current density (i_{corr}), the

Tafel slopes (β_c and β_a) and the causality factors (CF-2 and CF-3). These electrochemical parameters were listed in Table (8). The data presented in Table (8) obviously show that, the addition of any one of tested compounds at a given concentration to the acidic solution decreases the corrosion current density, indicating that these compounds inhibit the corrosion of SS in 1 M HCl through adsorption.
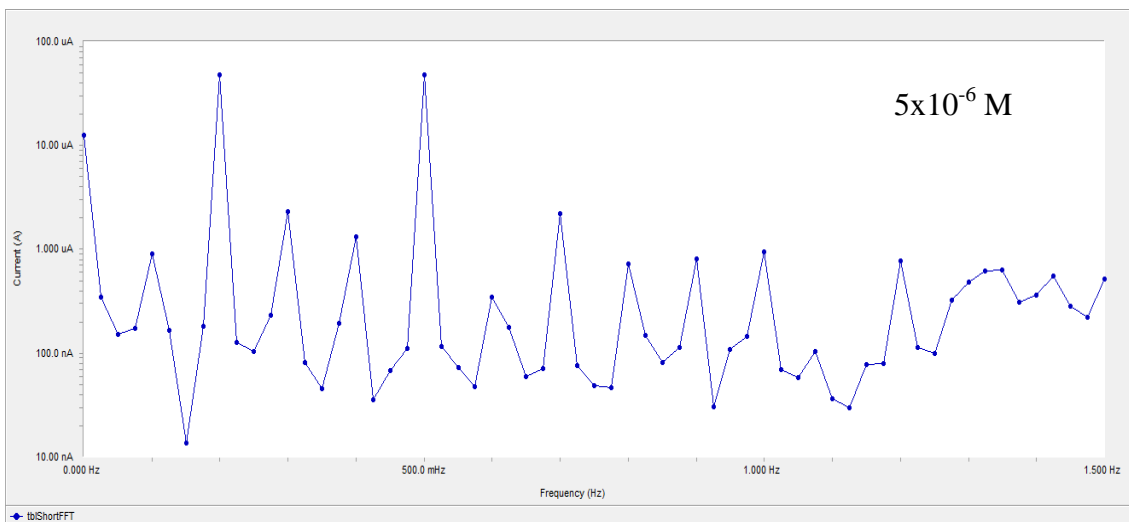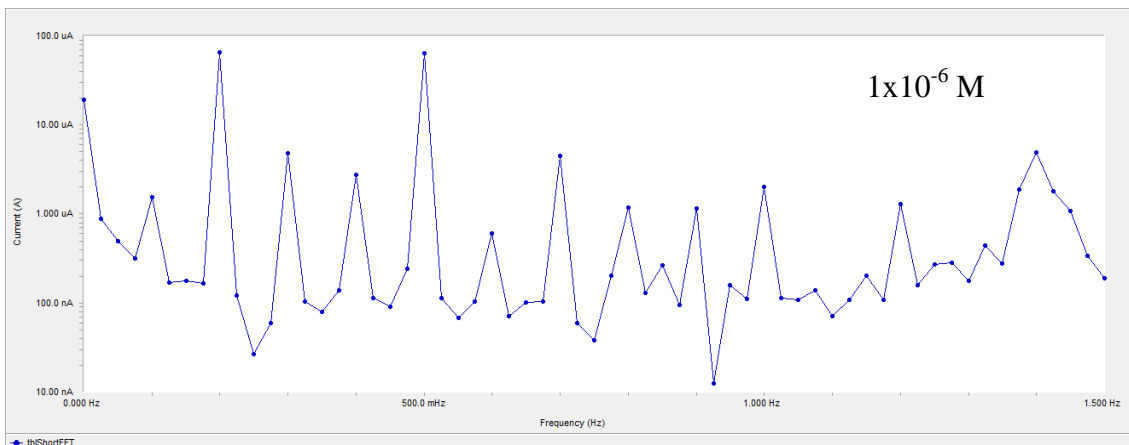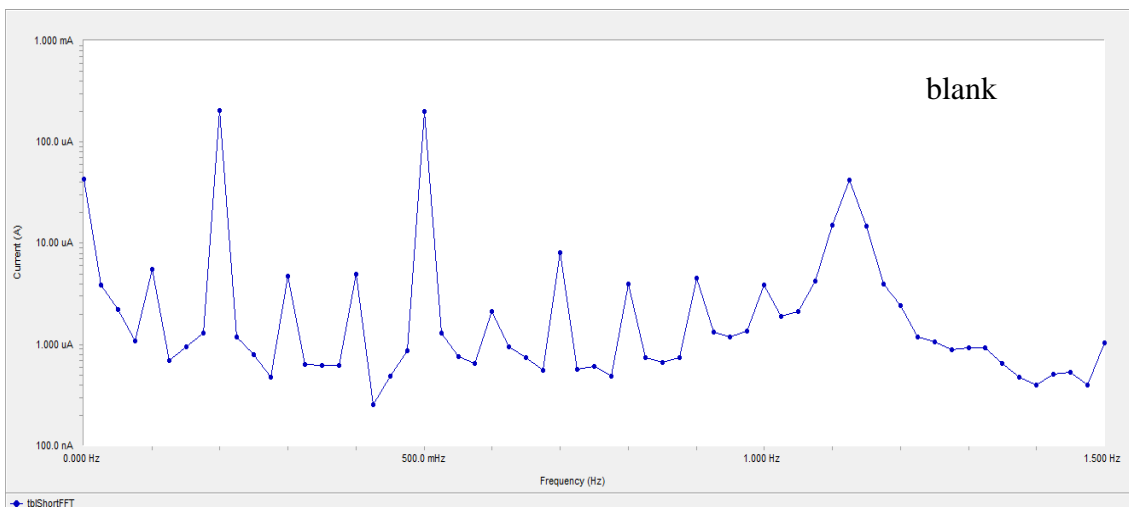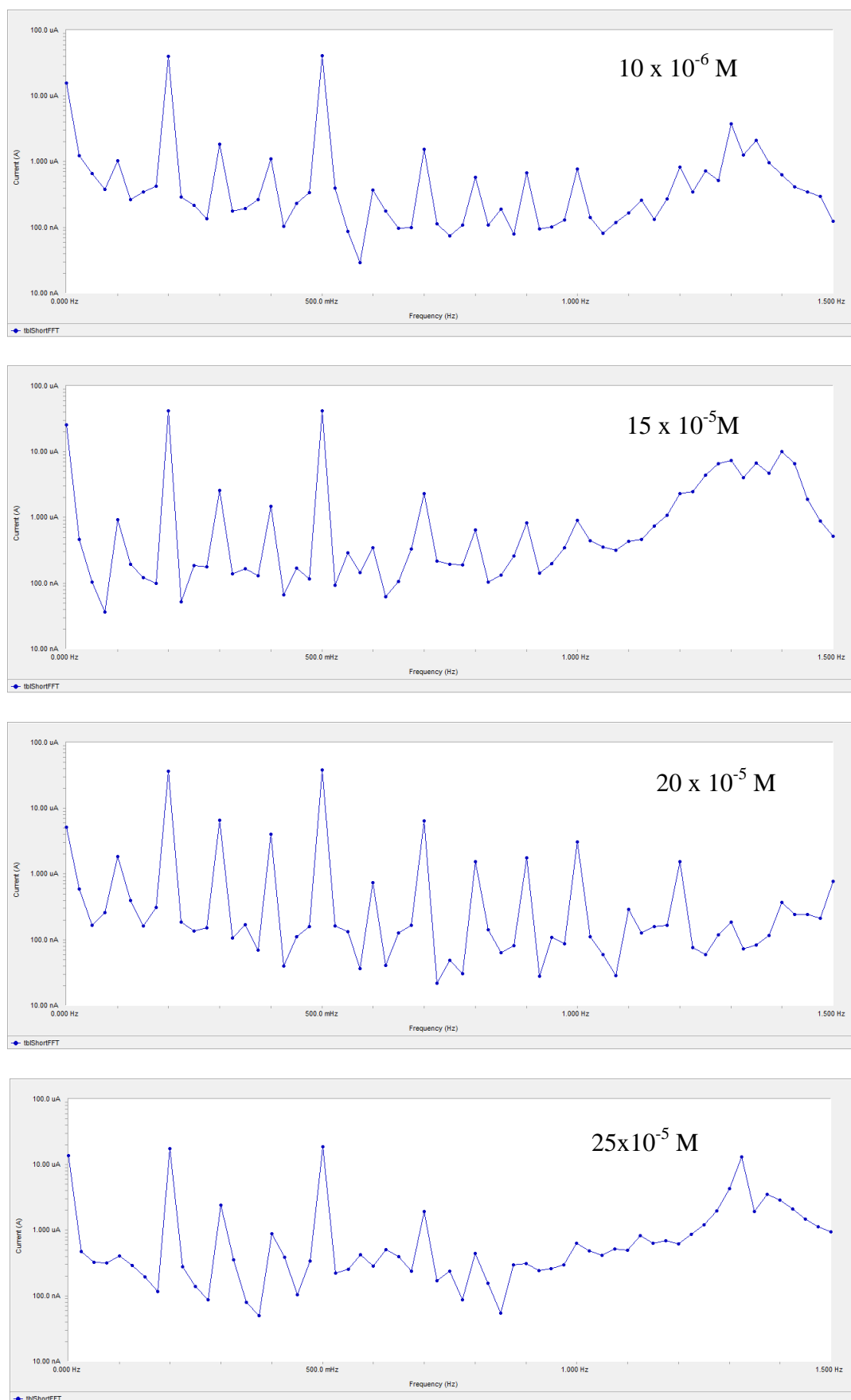
Figure 9. EFM spectra for SS type 304 in 1 M HCl in the presence and absence of different concentrations of compound (1) at 25˚C

The causality factors obtained under different experimental conditions are approximately equal to the theoretical values (2 and 3) indicating that the measured data are verified and of good quality [30]. The inhibition efficiencies % IE_{EFM} increase by increasing the studied inhibitor concentrations and was calculated from the equation:

$$\% \ IE_{EFM} = [(1 - i_{corr}/ i^{o}_{corr})] \times 100 \tag{12}$$

where i^{o}_{corr} and i_{corr} are corrosion current densities in the absence and presence of inhibitor, respectively. The inhibition sufficiency obtained from this method is in the order: compound (1) > compound (2).

Table 8. Electrochemical kinetic parameters obtained from EFM technique for SS type 304 in 1 M HCl in the absence and presence of different concentrations of compounds 1and 2 at 25°C

| Comp.	Conc., M	i_{corr} $\mu A \ cm^{-2}$	β_c $mVdec^{-1}$	β_a $mVdec^{-1}$	CF-2	CF-3	CR mpy	θ	% IE
	Blank	253.2	88	75	1.9	2.9	115.7	-	-
1	1×10^{-6}	85.09	105	72	2.1	2.8	38.88	0.664	66.4
	5×10^{-6}	67.49	105	80	2.1	2.7	30.84	0.733	73.3
	10×10^{-6}	53.07	95	76	2.0	2.9	24.25	0.79	79.0
	15×10^{-6}	45.56	81	63	2.0	3.0	20.82	0.820	82.0
	20×10^{-6}	36.48	96	47	1.9	2.9	16.67	0.856	85.6
	25×10^{-6}	23.11	119	64	2.1	2.8	10.56	0.908	90.8
2	1×10^{-6}	92.42	98	77	2.0	2.8	42.23	0.635	63.5
	5×10^{-6}	77.38	117	78	1.9	2.9	35.36	0.694	69.4
	10×10^{-6}	60.15	102	77	1.8	2.8	27.48	0.762	76.2
	15×10^{-6}	50.11	101	72	2.0	2.7	22.91	0. 802	80.2
	20×10^{-6}	41.93	85	64	2.0	2.7	19.16	0.834	83.4
	25×10^{-6}	36.48	101	75	2.1	2.8	16.67	0.850	85.0

3.5. Scanning Electron Microscopy (SEM) measurements

Figure (10) represents the micrography obtained for SS type 304 samples in presence and in absence of 25 x 10^{-5} M Chalcones derivatives after exposure for 3 days immersion. It is clear that SS type 304 surfaces suffer from severe corrosion attack in the blank sample. It is important to stress out

that when the compound is present in the solution, the morphology of SS type 304 surfaces is quite different from the previous one, and the specimen surfaces were smoother. We noted the formation of a film which is distributed in a random way on the whole surface of the SS type 304. This may be interpreted as due to the adsorption of the Chalcones derivatives on the SS type 304 surface incorporating into the passive film in order to block the active site present on the carbon steel surface. Or due to the involvement of inhibitor molecules in the interaction with the reaction sites of SS type 304 surface, resulting in a decrease in the contact between carbon steel and the aggressive medium and sequentially exhibited excellent inhibition effect [31, 32].
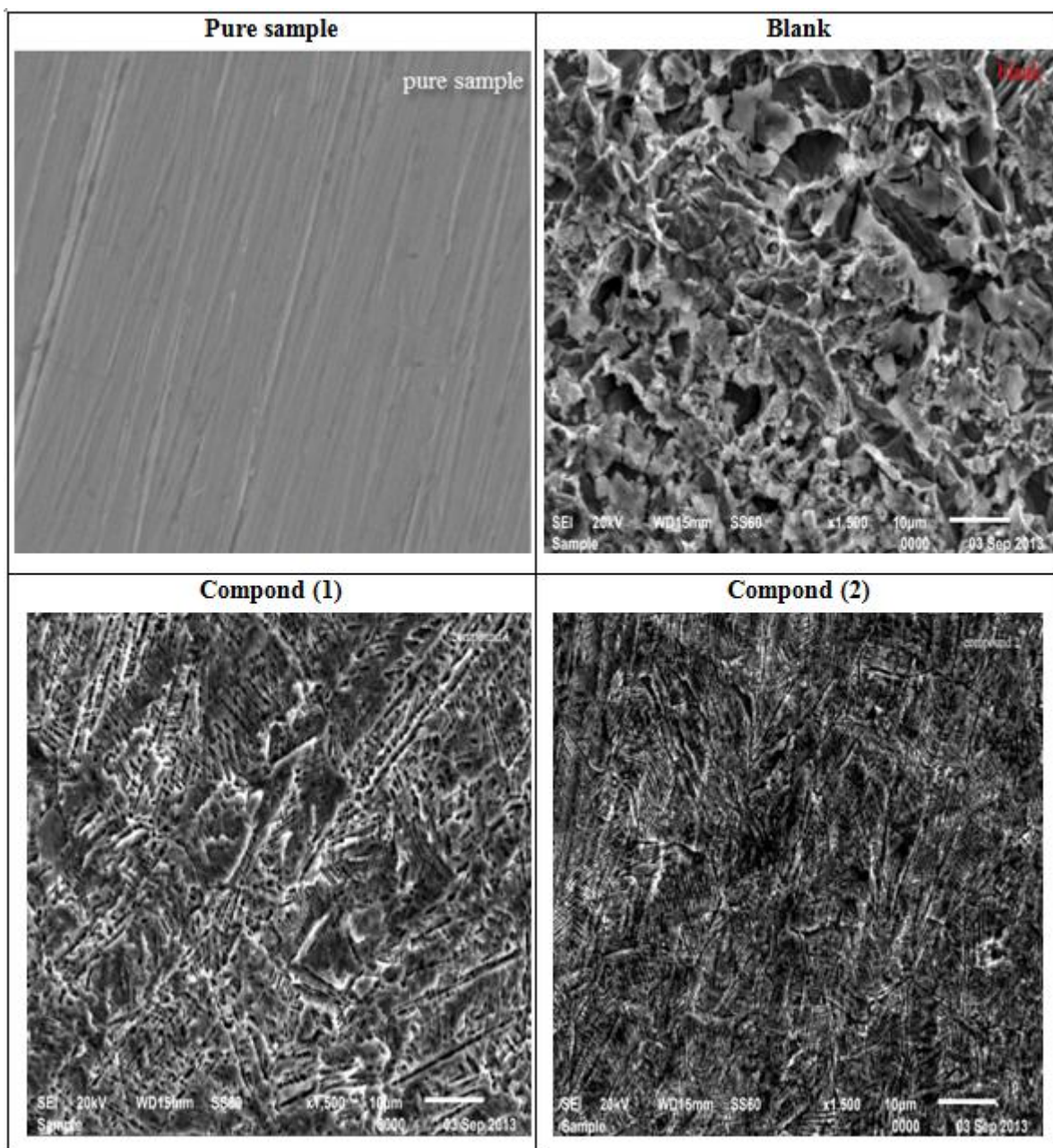
Figure 10. SEM micrographs for SS type 304 in absence and presence of 25×10^{-5} M of investigated compounds

3.6. Energy Dispersion X-ray Spectroscopy (EDX) measurements
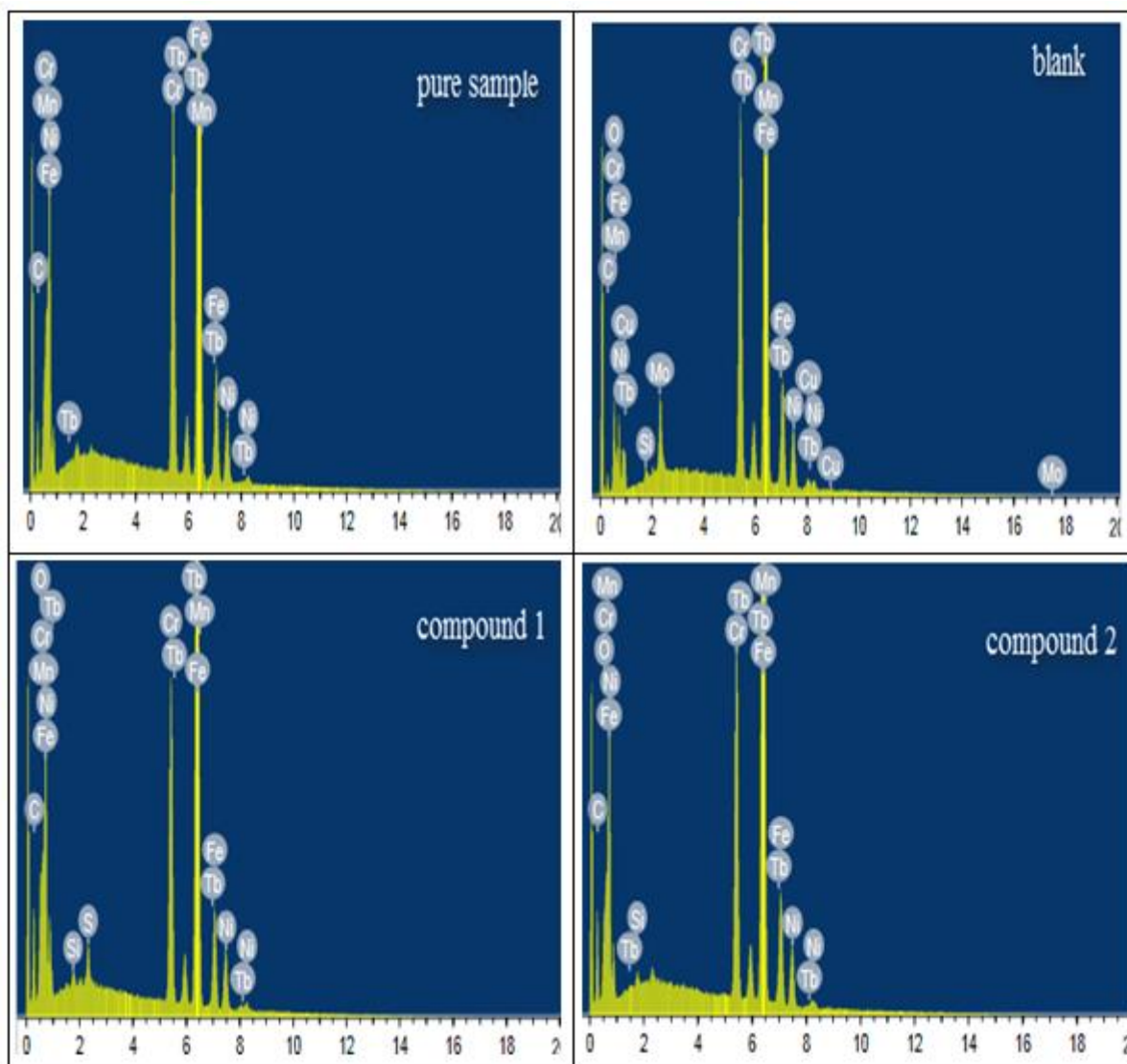
Figure 11. EDX analysis for SS type 304 absence and presence of 25×10^{-5} M of investigated compounds for 3 days immersion

The EDX spectra were used to determine the elements present on the surface of SS type 304 and after 3 days of exposure in the uninhibited and inhibited1 M HCl. Figure (11) shows the EDX analysis result on the composition of SS type 304 only without the acid and inhibitor treatment. The EDX analysis indicates that only Fe and oxygen were detected, which shows that the passive film contained only Fe_2O_3. Figure (11) portrays the EDX analysis of SS type 304 in 1 M HCl only and in the presence of 25×10^{-5} M of tested   derivatives. The spectra showed additional lines, demonstrating the existence of C (owing to the carbon atoms of tested derivatives). These data shows that the carbon and O atoms covered the specimen surface. This layer is entirely owing to the inhibitor, because the carbon and O signals are absent on the specimen surface exposed to uninhibited HCl. It is seen that, in

addition to Mn, C. and O were present in the spectra. A comparable elemental distribution is shown in Table (9).
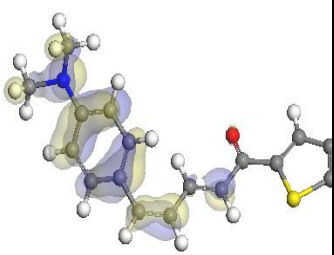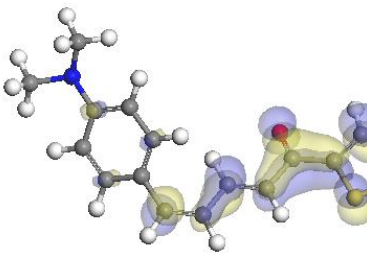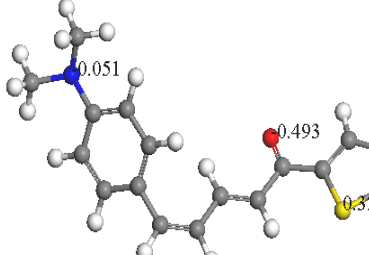
Table 9. Surface composition (weight %) of SS type 304 after 3days of immersion in 1 HCl without and with the optimum concentrations of the studied inhibitors

| (Mass %)	Fe	Mn	C	O	Cr	S	Tb
Pure	60.62	1.10	9.91	----	16.78	----	7.23
Blank	52.06	0.81	0.65	1.56	15.48	-----	----
Compound (1)	59.54	1.02	9.07	2.79	16.06	0.71	6.82
Compound (2)	56.87	0.99	7.79	2.06	15.85	-----	6.77

3.7. Quantum chemical calculations

Theoretical calculations were performed for only the neutral forms, in order to give further insight into the experimental results. Values of quantum chemical indices such as energies of LUMO and HOMO (E_{HOMO} and E_{LUMO}), dipole moment (μ) and energy gap ΔE, are calculated by semi-empirical PM3 method has been given in Table (10). The reactive ability of the inhibitor is related to E_{HOMO}, E_{LUMO}[33]. Higher E_{HOMO} of the adsorbent leads to higher electron donating ability. Low E_{LUMO} indicates that the acceptor accepts electrons easily. The calculated quantum chemical indices (E_{HOMO}, E_{LUMO}, μ) of investigated compounds are shown in Table (10). The difference $\Delta E = E_{LUMO} - E_{HOMO}$ is the energy required to move an electron from HOMO to LUMO. Low ΔE facilities adsorption of the molecule and thus will cause higher inhibition efficiency.

The bond gap energy ΔE increases from (1 to 2). This fact explains the decreasing inhibition efficiency in this order (1>2), as shown from Table (10) and Figure (12) show the optimized structures of the three investigated compounds. So, the calculated energy gaps show reasonably good correlation with the efficiency of corrosion inhibition. Table (10) also indicates that compound (1) possesses the lowest total energy that means that compound (1) adsorption occurs easily and is favored by the highest softness. The HOMO and LUMO electronic density distributions of these molecules were plotted in Figure (12). For the HOMO of the studied compounds that the benzene ring, N-atoms and O-atom have a large electron density.

Structure	HOMO	LUMO	Mulliken charges
1			
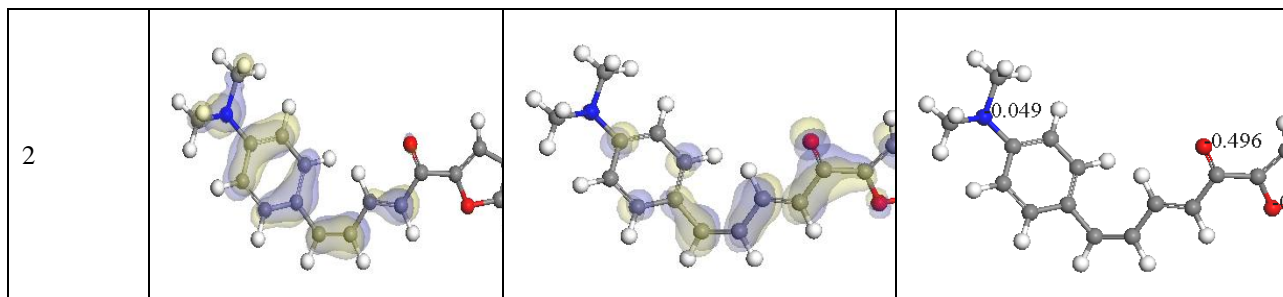
Figure 12. Molecular orbital plots and Mulliken charges of organic compounds

The data presented in Table (10) show that the calculated dipole moment decrease from compound (1) > compound (2).

Table 10. The calculated quantum chemical parameters for investigated compounds by using PM3

	Compound (1)	Compound (2)
$-E_{HOMO}$ (eV)	8.707	8.786
$-E_{LUMO}$ (eV)	1.323	1.200
ΔE (eV)	7.384	7.586
Dipole moment, μ, (Debye)	3.588	2.470
Molecular Area (Å^2)	323.564	314.910

3.8. Chemical structure of the inhibitors and corrosion inhibition

Inhibition of the corrosion of SS type 304 in 1M HCl solution by some Chalcones compounds is determined by weight loss, potentiodynamic anodic polarization measurements, electrochemical impedance spectroscopy (EIS), electrochemical frequency modulation method (EFM) and scanning electron microscopy (SEM) Studies, it was found that the inhibition efficiency depends on concentration, nature of metal, the mode of adsorption of the inhibitors and surface conditions. The observed corrosion data in presence of these inhibitors, namely: i) The decrease of corrosion rate and corrosion current with increase in concentration of the inhibitor, ii) The linear variation of weight loss with time, iii) The shift in Tafel lines to higher potential regions, iv) The decrease in corrosion inhibition with increasing temperature indicates that desorption of the adsorbed inhibitor molecules takes place and v) The inhibition efficiency was shown to depend on the number of adsorption active centers in the molecule and their charge density. It was concluded that the mode of adsorption depends on the affinity of the metal towards the π-electron clouds of the ring system. Metals such as Cu and Fe, which have a greater affinity towards aromatic moieties, were found to adsorb benzene rings in a flat orientation. The order of decreasing the percentage inhibition efficiency of the investigated inhibitors in the corrosive solution was as follow: compound (1) > compound (2). Compound (1) exhibits excellent inhibition power due to its larger molecular size that may facilitate better surface coverage,

and its adsorption through sulphur atom in thiophene ring. Compound (2) comes after compound (1) in inhibition efficiency due to its lower molecular size than compound (1) and contain furan ring in which oxygen atom is less adsorption than sulphur atom which present in thiophene ring in compound (1)

References

1. A.J. Szypowski, *Br. Corros. J*. 37 (2002) 141.
2. M.A. Quraishi, F.A. Ansari, D. Jamal, *Mater. Chem. Phys*. 77 (2003) 687.
3. M.Elachouri, M.S.Hajji, S.Kertit, E.M.Essassi, M.Salem and R.Coudert, *Corros.Sci*., 37 (1995) 381.
4. B.Merari, H.Elattar, M.Traisnel, F.Bentiss and M.Larenee, *Corros.Sci.*, 40 (1998) 391.
5. F.Bentiss, M.Traisnel, M.Lagrenee, *Corros.Sci.,* 42 (2000) 127.
6. L.Elkadi, B.Mernari,M.Traisnel, F.Bentiss and M.Lagrenee, *Corros.Sci*., 42 (2000) 703.
7. R.Walker, corros.Sci., 31 (1975) 97.
8. F.Bentiss, M.Lagrenee, M.Traisnel and J.C.Lornez, *Corros.Sci.,* 41 (1999) 789.
9. A. El-Kanouni, S. Kertti, A. Srhiri, K. Bachir, *Bull. Electrochem*.12 (1996) 517.
10. J.D.Talati and R.M.Modi, *Trans.SEAST*, 11 (1986) 259.
11. R. W. Bosch, J. Hubrecht, W. F. Bogaerts, B. C. Syrett, *Corrosion* 57 (2001) 60.
12. S. S. Abdel–Rehim, K. F. Khaled, N. S. Abd–Elshafi, *Electrochim. Acta*51 (2006) 3269.
13. Tomasz Tronina, AgnieszkaBartmańska, BeataFilip-Psurska, Joanna Wietrzyk, Jarosław Popłoński, EwaHuszcza, *Bioorganic& Medicinal Chemistry* 21 (7) (2013) 2001.
14. Z.Szklarska-Smiaiowska; Electrochemical and Optical Techniques for the Study of   Metallic Corrosion, Kluwer Academic, the Netherlands; (1991) 545.
15. I.Langmuir, *J.Amer.Chem.Soc*., 39 (1947) 1848.
16. E.Khamis, *Corrosion,* 46 (1990) 476.
17. G. Trabanelli, in "Corrosion Mechanisms" (Ed. F. Mansfeld) Marcel Dekker, New York, 119 (1987).
18. F.H. Asaf, M. Abou- Krisha, M. Khodari, F. EL-Cheihk, A. A. Hussien, *Mater Chem. Phys*., 93 (2002) 1.
19. A.Fiala, A. Chibani, A. Darchen, A. Boulkamh, K. Djebbar, *Appl. Surf. Sci*. 253(2007) 9347.
20. S.T. Arab and E.M. Noor, Corrosion 49 (1993) 122.
21. W. Durnie, R.D. Marco, A. Jefferson, B. Kinsella, *J. Electrochem. Soc*., 146 (1999) 1751.
22. J. M. Thomas and W. J. Thomas, Introduction to the Principles of Heterogeneous Catalysis, 5th, Ed, Academic Press, London (1981) 14.
23. A. El-Ouafi, B. Hammouti, H. Oudda, S. Kerit, R. Touzani, A. Ramdani, *Anti-Corros. Meth. Mater* .49 (2002) 199.
24. F. Mansfeld, M.W. Kendig, S. Tsai, *Corrosion,* 38 (1982) 570.
25. F. Mansfeld, *Eletrochim. Acta*, 35 (1990) 1533.
26. E. McCafferty, N Hackerman, *J. Electrochem. Soc.* 119 (1972) 146.
27. E. Kus, F. Mansfeld, *Corros. Sci.* 48 (2006) 965.
28. G. A. Caigman, S. K. Metcalf, E. M. Holt, *J.Chem. Cryst*.30 (2000) 415.
29. D.C. Silverman and J.E. Carrico, *National Association of Corrosion Engineers*, 44 (1988), 280.
30. R.A., Prabhu, T.V., Venkatesha, A.V., Shanbhag, G.M., Kulkarni, R.G., alkhambkar,*Corros.Sci.,* 50 (2008) 3356
31. G., Moretti, G., Quartanone, A., Tassan, A., Zingales, ,*Wekst. Korros.,*45(1994) 641
32. C. Lee, W. Yang and R. G. Parr., *Phys. Rev. B*, 37 (1988) 785.
33. R. M. Issa, M. K. Awad and F. M. Atlam, *Appl. Surf. Sci.,* 255 (2008) 2433